Environ. Sci. Technol. **2007**, *41,* 1405−1412

Using Bromine Gas To Enhance Mercury Removal from Flue Gas of Coal-Fired Power Plants

SHOU-HENG LIU,[†,§] NAI-QIANG YAN,[†,⊥] ZHAO-RONG LIU,[†,∥] ZAN QU,[†,⊥] H. PAUL WANG,[†,§] SHIH-GER CHANG,*[,†] AND CHARLES MILLER[‡]

Environmental Energy Technology Division, Lawrence Berkeley National Laboratory, University of California, Berkeley, California 94720, and National Energy Technology Laboratory, Pittsburgh, Pennsylvania 15236

Bromine gas was evaluated for converting elemental mercury (Hg^0) to oxidized mercury, a form that can readily be captured by the existing air pollution control device. The gas-phase oxidation rates of Hg^0 by Br_2 decreased with increasing temperatures. SO_2, CO, HCl, and H_2O had insignificant effect, while NO exhibited a reverse course of effect on the Hg^0 oxidation: promotion at low NO concentrations and inhibition at high NO concentrations. A reaction mechanism involving the formation of van der Waals clusters is proposed to account for NO's reverse effect. The apparent gas-phase oxidation rate constant, obtained under conditions simulating a flue gas without flyash, was 3.61×10^{-17} $cm^3 \cdot molecule^{-1} \cdot s^{-1}$ at 410 K corresponding to a 50% Hg^0 oxidation using 52 ppm Br_2 in a reaction time of 15 s. Flyash in flue gas significantly promoted the oxidation of Hg^0 by Br_2, and the unburned carbon component played a major role in the promotion primarily through the rapid adsorption of Br_2 which effectively removed Hg^0 from the gas phase. At a typical flue gas temperature, SO_2 slightly inhibited the flyash-induced Hg^0 removal. Conversely, NO slightly promoted the flyash induced Hg^0 removal by Br_2. Norit Darco-Hg-LH and Darco-Hg powder activated carbons, which have been demonstrated in field tests, were inferred for estimating the flyash induced Hg^0 oxidation by Br_2. Approximately 60% of Hg^0 is estimated to be oxidized with the addition of 0.4 ppm of gaseous Br_2 into full scale power plant flue gas.

Introduction

Coal-fired power plants represent a major anthropogenic mercury emission source (*1*). It has been estimated that U.S. coal-fired power plants currently emit approximately 48 tons of mercury per year (*2*), which accounts for about one-third of the mercury emission in the U.S. On March 18, 2005, the U.S. EPA issued the first Clean Air Mercury Rule (CAMR) for the control of mercury emissions from coal-fired power plants (*3*). The CAMR requires an overall average reduction in mercury emissions of about 69% by 2018.

Results on mercury speciation in flue gas of power plants indicate that some degree of mercury cobenefit control can be achieved by existing air pollution control devices (APCDs) (*2*). The extent of the mercury removal across existing APCDs can vary significantly depending on coal ranks, flyash properties, and APCD configurations. Mercury is present in flue gas in varying percentages in three basic forms (*4*): particulate-bound mercury, elemental (Hg^0), and oxidized mercury in gas form. The particulate-bound mercury can be easily removed by ESP or fabric filters (*5*). The oxidized mercury has a tendency to stick to particulate matter and is water soluble (*6*). Consequently, it can be captured by the ESP, fabric filters, or FGD. Conversely, Hg^0 is highly volatile and insoluble in water and is thus not readily removed by existing APCDs.

Although conventional APCDs can capture some mercury, new mercury control technologies (*2*, *7*) will be needed to help achieve the level of control necessary to meet the mercury emission cap. Given the fact that the oxidized mercury can be readily captured by the APCDs, a logical approach is to find a cost-effective method to increase Hg^0 oxidation ahead of the APCDs.

In general, power plants burning bituminous coals demonstrate significantly higher mercury capture than similarly equipped subbituminous- and lignite-fired plants. The higher performance observed for bituminous coals has been linked to higher levels of the oxidized mercury associated with the coal's high chlorine content (*2*). Research has been conducted by many investigators to elucidate the mechanisms of mercury oxidation involving chlorine species (*8*).

Hg^0 is a large atom with 80 electrons moving around its nucleus. As a result, it is highly polarizable, and the London dispersion forces should play an important role in its interaction with surrounding atoms and molecules. The London dispersion forces increase greatly as the size of the atom or nonpolar molecule increases (*9*). Br_2 has 70 electrons compared to 34 electrons on Cl_2. It is expected that Br_2 is more effective than Cl_2 for Hg^0 oxidation. The gas-phase oxidation of Hg^0 by Br_2 has been studied (*10*) but not under the flue gas conditions.

This paper reports an investigation of the oxidation rate of Hg^0 by Br_2 under flue gas conditions downstream from the air heater and upstream from the particulate collectors and determines the potential of using Br_2 gas for the enhancement of mercury removal from flue gas of coal-fired power plants.

Experimental Section

The kinetics of the reaction were investigated by monitoring the concentration of Hg^0 as a function of time in Pyrex flasks by a mercury cold vapor atomic absorption spectrophotometer (CVAAS) (*11*). Three sizes of flasks with different surface-to-volume ratios (190 cm^2/190 mL, 255 cm^2/380 mL, and 498 cm^2/960 mL) were employed to determine the contributions of surface catalyzed reactions (*11*).

The reaction was performed using the absolute rate technique under pseudo-first-order conditions (*12*) with respect to Hg^0. The Hg^0 concentrations employed were 0.01 ppm−0.20 ppm, with Br_2 present in considerable excess, ranging between 4 and 60 ppm. Therefore, the concentrations

* Corresponding author phone: (510)486-5125; fax: (510)486-7303; e-mail: sgchang@lbl.gov.
† Lawrence Berkeley National Laboratory.
‡ National Energy Technology Laboratory.
§ On leave from the Environmental Engineering Department, National Cheng Kung University, Tainan 70101, Taiwan.
⊥ On leave from the School of Environmental Science and Engineering, Shanghai Jiao Tong University, Shanghai 200240, People's Republic of China.
∥ On leave from the Center of Environmental Sciences, Peking University, Beijing 100871, People's Republic of China.

10.1021/es061705p CCC: $37.00
Published on Web 01/18/2007

of Br_2 remained almost constant during the entire course of the reaction.

The flask wall surface was coated with a halocarbon wax (HC) to minimize adsorption and catalytic effects (*11*), while the photon interference (*11*) was minimized by blocking UV light from entering the flask during most of the course of the reaction. The photons excite some of Hg^0 from the ground state to the excited states, which could be oxidized by Br_2 at a different rate.

Each run was conducted by evacuating the flask, and then a volume of N_2 saturated with Hg^0 vapor was injected to the flask using a syringe until the pressure of the flask reached about 250 Torr. A volume of a known concentration of Br_2 in N_2 was then injected by syringe into the flask, and the pressure was quickly brought to 760 Torr with nitrogen. The procedure of introducing gas reactants into a flask mentioned above improves gas mixing and minimizes the mass transfer effect due to gas diffusion.

To investigate the effect of flue gas components on the oxidation of Hg^0 by Br_2, a volume of SO_2, NO, CO, HCl, and/or H_2O vapor in N_2 was introduced to the flask by syringe before Br_2 was added. To study the effect of flyash, the HC was heated to about 363 K to form a fluid, which was then painted onto the inner wall of the flask with a brush. The flask was then heated in an oven and rotated around to ensure a complete and even coating on the wall. A weighted amount of flyash was then sprayed into the flask (*12*), while the flask was at about 320 K when the HC was slightly sticky. Finally, the reactor was cooled to room temperature. The HC serves two purposes: minimizing the Pyrex-surface induced Hg^0 oxidation and holding the flyash in place on the inner wall of the flask. The average weight of the flyash on the wall was about 2.8 ± 0.3 mg/cm^2. Elemental analysis of flyash was performed by the energy dispersive X-ray spectroscopy. Elemental weight percents were 12.13 and 18.15 (Si); 10.35 and 12.96 (Ca); 9.88 and 12.79 (Al); 17.20 and 4.29 (Fe); 1.24 and 1.22 (K); 5.39 and 0.41 (S); and 12.4 and 1.3 (unburned carbon) for bituminous and lignite flyash, respectively, with the remaining oxygen and trace elements. Flasks coated with flyash were used for no more than 3 runs before being cleaned and reprepared to minimize the changes of flyash properties that could occur due to the deposition of products and/or reactants. Flyash and HC were removed from the flasks with chloroform after one to three experiments since mercury product on the surface was found to enhance Hg^0 capture (*11*). The accuracies of results of first three runs were within 20%. The loss on ignition (LOI) of flyash was determined by heating the sample in air to 750 °C for a period of several hours after which the weight change was recorded as LOI.

To investigate the adsorption kinetics of Br_2 on flyash, experiments were performed with a cylindrical gas cell. The cell wall was coated with flyash as described above. The concentration of Br_2 in the cell was determined based on its absorption of UV-visible light, with a molar extinction coefficient of 165 cm^3/mol·cm at 415 nm. The thermodynamics of the adsorption of Br_2 on flyash was studied with a 550 mL Pyrex flask containing about 2 g of flyash. After the introduction of Br_2 (50 ppm − 1%) into the flask in an oven at various temperatures, a gas sample was transferred by a syringe to a gas cell for determining the equilibrium concentration of Br_2.

The uncertainty of Hg^0 and Br_2 concentrations measured was ±0.005 ppm and <5%, respectively. The accuracy of the data reported here was estimated to be within 20%.

The chemicals employed were as follows: bromine (99.6%), mercury (99.99%), and chloroform (99.99%) from Sigma-Aldrich Co.; nitric oxide (>99%), carbon monoxide (9.8%), and sulfur dioxide (>99%) from Matheson Co.; halocarbon wax (HC, Series-1500) from Halocarbon Product Co.; and Darco-Hg and Darco-Hg-LH powder activated carbons (PAC) from Norit American. Bituminous (flyash-B) and lignite (flyash-L) flyash were provided by MobotechUSA.

Results and Discussion

The kinetics were performed using a large excess of oxidants, Br_2 or sorbent, over Hg^0. Under such a condition, the half-life of Hg^0, i.e. the time required for the concentration of Hg^0 to fall to one-half of its initial value, can be expressed as $t_{1/2} = \ln 2/k$[oxidants or sorbent] (*13*). Therefore, the half-life is independent of the initial Hg^0 concentration employed.

Wall and Light Effects. The half-life of Hg^0 due to the adsorption on Pyrex wall was more than 500 s without Br_2. The half-life decreases to 6.6 s with 13 ppm Br_2 at 296 K (Figure 1a). After the wall was coated with HC, there was no detectable adsorption of Hg^0 on the wall. Thus the results obtained with a HC coated flask should measure the actual gas-phase reaction kinetics. The half-life of Hg^0 was 29 s with HC coating compared to 6.6 s without the coating at 13 ppm Br_2. The Pyrex wall evidently promoted the oxidation of Hg^0 by Br_2.

The effect of 253.7 nm light on Hg^0 oxidation by Br_2 was studied. The results indicated that the photons displayed a small enhancement effect by about 5% on Hg^0 oxidation (Figure 1a) under the conditions employed.

From the aforementioned studies, it is clear that in order to avoid the wall and light effects, the kinetics of gas-phase oxidation of Hg^0 must be performed with a HC coated flask and under an intermittent illumination mode for Hg^0 concentration measurements.

Gas-Phase Oxidation of Hg^0 by Br_2. The Gibbs free energy of the reaction $Hg^0 + Br_2 \rightarrow HgBr_2$ is calculated to be −35.6 kcal/mol at 298 K and −30.8 kcal/mol at 500 K (*14*), indicating a thermodynamically favorable reaction. The disappearance of Hg^0 exhibited an exponential decay with time (Figure 1a), indicative of a pseudo-first-order reaction with respect to Hg^0

$$-\mathrm{d}[Hg^0]/\mathrm{d}t = k'[Hg^0] \quad (1)$$

where k' is the pseudo-first-order rate constant.

The rate constants, k', obtained from the Hg^0 concentration-time dependence curves, as a function of Br_2 concentration in three flasks were determined (Figure 1b). The results indicate that k' had a strong linear correlation with the $[Br_2]$, indicative of a first-order kinetics with respect to Br_2 concentrations. The small flask produced slightly larger values of k', which was attributed to the quartz window surface effect (*11*). The window's contribution would be more prominent in the small flask because of a larger surface to volume ratio. By conducting experiments at various Br_2 concentrations using different sizes of flasks, the contributions from three concurrent pathways, gas phase, HC coated wall, and window surface induced reactions, can be calculated (*11*). The results indicated that the effect of the HC coated wall was insignificant and that the window effect was more prominent in the small size flask and at low Br_2 concentrations. As mentioned above, the rate of the disappearance of Hg^0 was found to be first order with respect to the Br_2 concentration. Therefore, the rate law can be expressed as

$$-\mathrm{d}[Hg^0]/\mathrm{d}t = k[Hg^0][Br_2] \quad (2)$$

where $k = k'/[Br_2]$ and is the second-order gas-phase rate constant, and $[Br_2]$ is the bromine concentration in gas phase.

Our work determines k to be $6.0(\pm 0.5) \times 10^{-17}$ cm^3·molecules^{-1}·s^{-1} at 296 K and 760 Torr, which is within an upper limit of $9.0(\pm 1) \times 10^{-17}$ cm^3·molecules^{-1}·s^{-1} at 298 K determined previously (*10*). The rate constant of Hg^0 oxidation by Br_2 is more than 2 orders of magnitude larger than that by Cl_2 (*11*), supporting a stronger van der Waals interaction

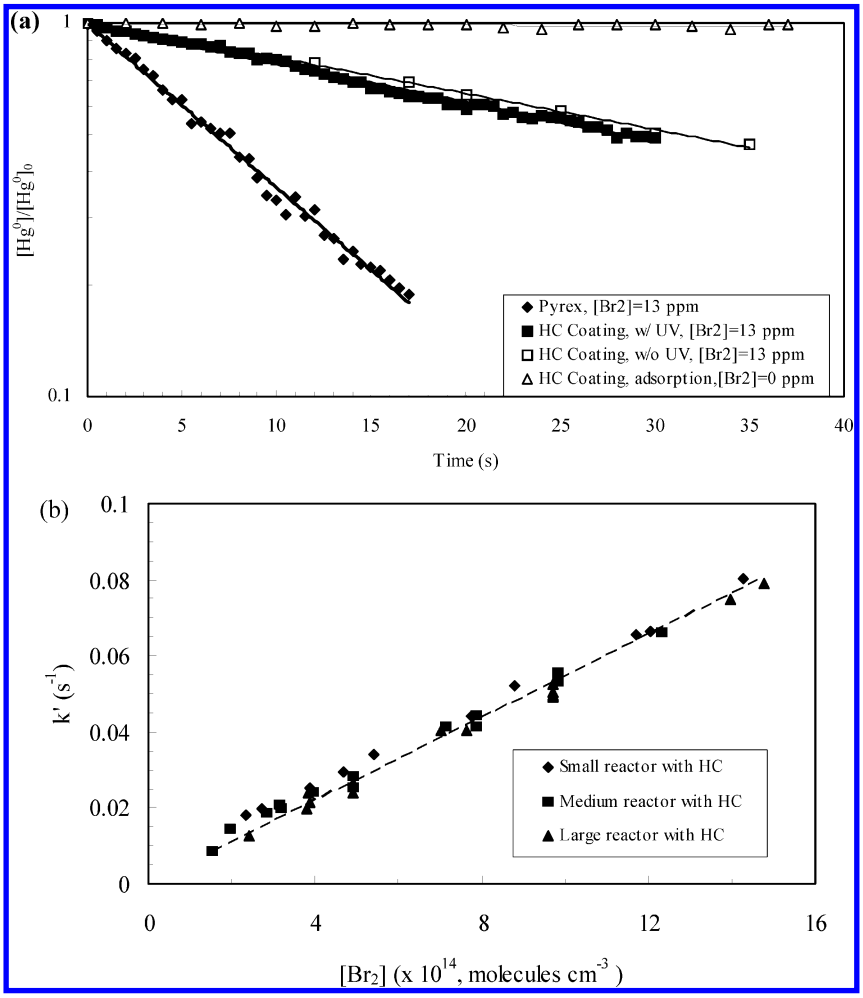

FIGURE 1. (a) The effect of wall, light, and/or Br_2 on the Hg^0 adsorption and oxidation rates at 296 K, where w/HC refers flask wall coated with the halocarbon wax; w/uv and w/o UV refer to experiments carried out with continuous and intermittent irradiation, respectively. The initial Hg^0 concentration was 0.2 ppm. (b) The pseudo-first-order rate constants of the reactions between Hg^0 and Br_2 determined at various Br_2 concentrations in three flasks with different surface to volume ratios at 296 ± 1 K.

of Hg^0 with Br_2 than Cl_2. The rate constants were determined between 298 K and 365 K and were found to decrease with increasing temperature as represented by eq 3, obtained from an Arrhenius graph by plotting ln k vs $1/T$ (*13*).

$$k = 4.7\ (\pm 0.5) \times 10^{-18} \exp\left[(760 \pm 80)/T\right] \qquad (3)$$

Effect of SO_2, NO, CO, HCl, and H_2O on Hg^0 Gas-Phase Oxidation. The oxidation rates of Hg^0 by Br_2 did not exhibit a detectable change in the presence of SO_2 (0−1300 ppm), CO (0−130 ppm), HCl (10 ppm), or O_2 (0−21%) in the temperature range studied (276−365 K). However, NO promoted the oxidation rate of Hg^0 by Br_2 at low NO concentration (<8 ppm) but inhibited the oxidation rate when NO was greater than 10 ppm (Figure 2).

The reaction mechanisms that can explain the reverse course of NO effect on Hg^0 oxidation by Br_2 were considered. The possibility that the promotion effect was due to the consumption of Hg^0 by NO is ruled out because there was no detectable reaction between Hg^0 and NO based on the UV measurement. Another possibility involving NO catalyzed generation of Br atoms, which subsequently reacted with Hg^0 to form HgBr species, was considered (*10*). However, the reaction $Hg^0 + Br_2 \rightarrow HgBr + Br$ has a large positive Gibbs free energy of 25.75 kcal/mol at 298 K and 24.46 kcal/mol at 500 K (*14*). Consequently, it is unlikely that Br atoms were involved under the conditions employed. On the other hand, the loss of Br_2 oxidant by reaction with NO, according to a three-body collision process: $Br_2 + 2NO \rightarrow 2NOBr$ having a rate constant (*15*) of 2.91×10^{-38} cm^6/molecule^2 s at 333 K, is too slow to account for the inhibition behavior observed.

After ruling out the aforementioned possibilities, the reaction mechanisms involving van der Waals clusters were proposed to explain the observed phenomenon. The major elementary reactions include

$$Hg^0 + Br_2 \leftrightarrow HgBr_2^* \qquad (4)$$

$$HgBr_2^* + M \rightarrow HgBr_2 + M \qquad (5)$$

$$HgBr_2^* + NO \rightarrow Hg^0 + Br_2 + NO \qquad (6)$$

$$NO + Br_2 \leftrightarrow NOBr_2^* \qquad (7)$$

$$Hg^0 + NOBr_2^* \rightarrow HgBr_2 + NO \qquad (8)$$

As mentioned above, both Hg^0 and Br_2 have large diffuse electron clouds and are highly polarizable. They are attracted to each other by London forces, resulting in the formation of $HgBr_2^*$ van der Waals clusters (eq 4). $HgBr_2^*$ relaxed to form a stable $HgBr_2$ molecule after colliding with a third molecule M, such as N_2 (eq 5). However, $HgBr_2^*$ could be separated into Hg^0 and Br_2 upon the electrostatic interaction with NO, a molecule with an unpaired electron (eq 6). Similarly, $NOBr_2^*$ van der Waals cluster was formed as a result

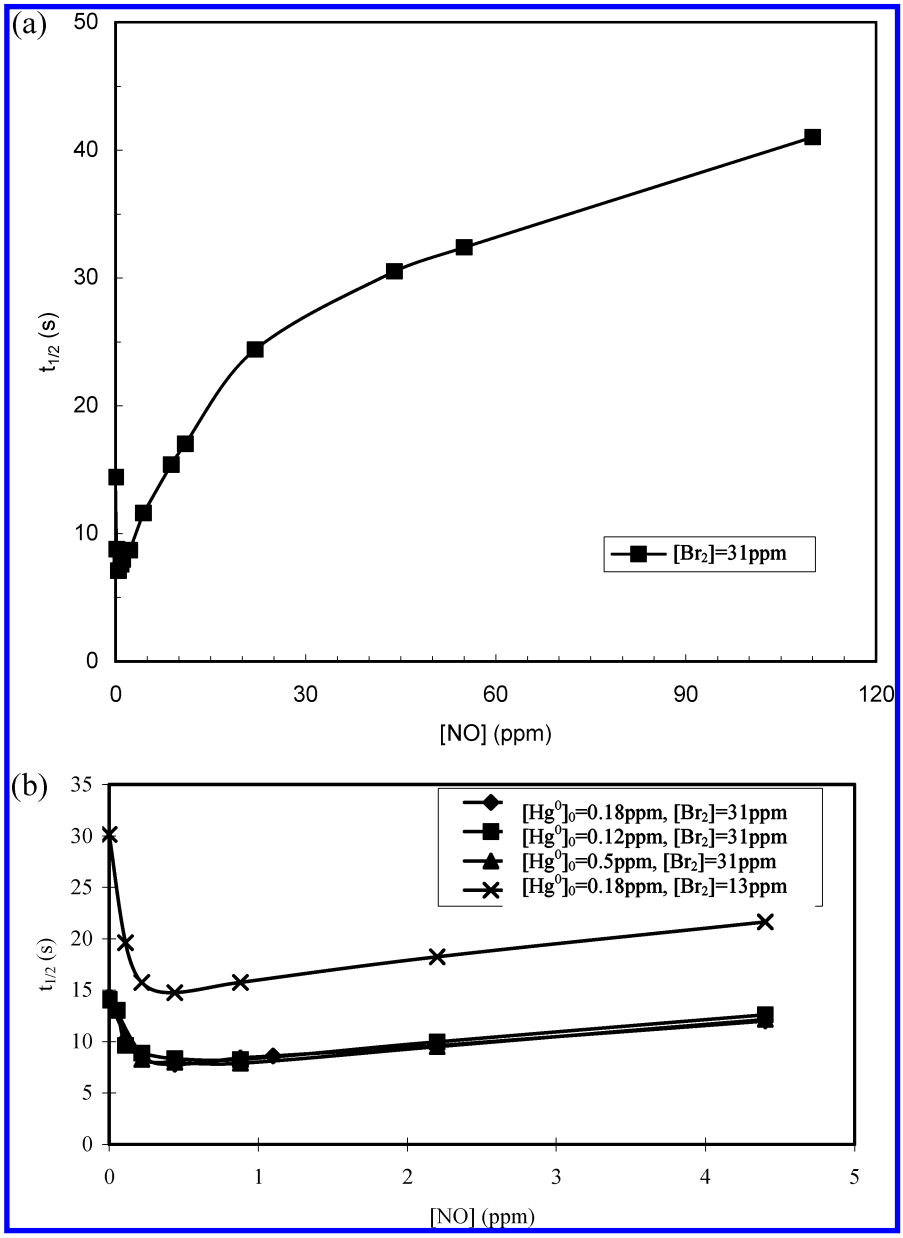

FIGURE 2. The reverse effect of NO on Hg^0 oxidation by Br_2 at 296 K. The Hg^0 half-life was plotted as a function of NO concentrations. (a) Rate inhibition at NO >10 ppm and (b) rate promotion at NO < 10 ppm.

of the interaction of the polarizable Br_2 with NO (eq 7). Collision of Hg^0 with $NOBr_2$* provided another route for the production of $HgBr_2$ (eq 8). The formation of the $HgBr_2$* (eq 4) and $NOBr_2$* (eq 7) were assumed to be in fast equilibrium. Based on the mechanisms proposed and under the steady-state conditions, the rate of the formation of $HgBr_2$ can be derived:

$$d[HgBr_2]/dt = \frac{k_4 k_5 [M][Hg^0][Br_2]}{k_{-4} + k_5[M] + k_6[NO]} + \frac{k_7 k_8 [Hg^0][Br_2][NO]}{k_{-7} + k_8[Hg^0]} \quad (9)$$

When [NO] is small, such that $k_{-4} + k_5[M] \gg k_6[NO]$, the influence of [NO] on the first term is negligible, while the second term shows an increase in the $HgBr_2$ formation rate with an increase of [NO]. This explains the increase of the disappearance rate of Hg^0 with an increase of [NO].

Further increase of [NO] would result in a reduction of $HgBr_2$ formation in the first term. When the magnitude of this reduction is greater than the increase from the second term, the overall $HgBr_2$ formation rate would exhibit a slow down. Although the proposed mechanisms can account for the experimental observation under the conditions employed, the fundamental chemical dynamics involving NO is the subject of a separate study and is not the main purpose of this investigation. Under most flue gas conditions, NO is expected to have concentrations large enough to exhibit the inhibition effect. Inhibition behavior was also observed with NO_2, another molecule with odd number of electrons. The inhibition effect was not observed for molecules with an even number of electrons such as SO_2, CO, and O_2.

The half-life of Hg^0 showed little effect in the presence of 5% H_2O compared to the case without H_2O at 363 K. Given that the temperature of the flue gas upstream from the particulate collector is greater than 390 K, H_2O vapor should not pose a significant effect on Hg^0 oxidation.

Effect of Flyash on the Oxidation of Hg^0 by Br_2. Four types of flyash, including bituminous flyash (flyash-B), lignite flyash (flyash-L), bituminous flyash without unburned carbon (flyash-B0), and lignite flyash without unburned carbon

TABLE 1. Adsorption Equilibrium Constants and the Maximum Adsorption Capacity[a] of Br_2 on Flyash at Various Temperatures

	flyash rank							
	flyash-L			flyash-B			flyash-L0	
parameters	296 K	365 K	413 K	296 K	365 K	413 K	296 K	365 K
K, cm^2·molecules^{-1}	6.1×10^{-17}	5.6×10^{-17}	5.3×10^{-17}	5.5×10^{-17}	5.1×10^{-17}	4.9×10^{-17}	6.8×10^{-17}	5.7×10^{-17}
$[Br_2]_{sm}$, molecules·g^{-1}	4.5×10^{19}	2.9×10^{19}	2.4×10^{19}	5.7×10^{19}	3.9×10^{19}	3.1×10^{19}	5.9×10^{17}	1.8×10^{17}

[a] The data accuracies were within 5% due to the uncertainty of $[Br_2]$ measurements.

(flyash-L0), were studied for the Hg^0 adsorption capacity and the catalytic oxidation of Hg^0 by Br_2. The LOI is the loss on ignition of the unburned carbon in flyash. Flyash without unburned carbon represents flyash with unburned carbon removed by heat treatment. For comparison, two PAC samples, Darco-Hg and Darco-Hg-LH, were tested under the same experimental conditions.

LOI and BET surface areas, respectively, were measured to be 12.4% (wt) and 11.35 m^2/g for flyash-B; 0% and 1.41 m^2/g for flyash-B0; 1.3% and 6.56 m^2/g for flyash-L; and 0% and 1.40 m^2/g for flyash-L0. The BET surface area of unburned carbon in bituminous and lignite flyash is calculated to be 81 m^2/g and 398 m^2/g, respectively. These results obviously suggest that the surface area of unburned carbon in flyash may vary depending on the type of coal burned.

To obtain the rate of flyash-induced Hg^0 oxidation by Br_2, the baseline information on the adsorption kinetics of Br_2 and Hg^0 on flyash must be obtained beforehand.

Adsorption of Br_2 on Flyash. The Br_2 adsorption kinetics on flyash was too fast to study with the apparatus employed. The adsorption took place and reached the equilibrium almost instantaneously (within 2 s). Nevertheless, the Langmuir adsorption isotherm (*16*) of Br_2 on flyash-B, flyash-L, and flyash-L0 at 296 K, 365 K, and 413 K was obtained (Table 1)

$$\theta = [Br_2]_s/[Br_2]_{sm} = K[Br_2]/(1 + K[Br_2]) \quad (10)$$

where θ is the fraction of the adsorption sites covered by Br_2; $[Br_2]_s$ is the amount of the adsorbed Br_2 on flyash; $[Br_2]_{sm}$ is the maximum adsorption capacity of Br_2 on flyash; and $[Br_2]$ is the concentration of Br_2 in gas phase. K is the equilibrium constant of adsorption.

As expected, the flyash samples exhibited a decrease of $[Br_2]_{sm}$ and K with an increase of temperature. Also, it was found that $[Br_2]_{sm}$ of flyash-L0 was 2 orders of magnitude smaller than that of flyash-L, indicating that the adsorption of Br_2 was mainly on the unburned carbon portion of the flyash. The greater adsorption capacity of Br_2 on the unburned carbon in flyash-L is attributed to a much larger surface area of unburned carbon in flyash-L than in flyash-B.

From the mass balance of Br_2, the following equation can be obtained

$$[Br_2]_0 = [Br_2] + (M/V)[Br_2]_s \quad (11)$$

where $[Br_2]_0$ is the initial Br_2 concentration in the gas phase; M is the amount of flyash; and V is the volume of the gas.

From eqs 10 and 11, the concentration of Br_2 in the gas phase, $[Br_2]$, and the amount of the adsorbed Br_2 on flyash, $[Br_2]_s$, at equilibrium conditions can be calculated if the initial concentration of Br_2, $[Br_2]_0$, introduced into the duct is known.

Adsorption of Hg^0 on Flyash. The experiments were performed without Br_2 and flue gas active components in the flasks. The disappearance of Hg^0 exhibited an exponential decay. The half-life ($t_{1/2}$) of Hg^0 was 214 s with flyash-B, 680 s with flyash-B0, 205 s with flyash-L (Table 2), and 560 s with flyash-L0 at 358 K. The results clearly indicate that the unburned carbon in flyash plays a major role in Hg^0 adsorption. The long half-lives imply that the adsorption of Hg^0 on flyash alone should not contribute significantly to the removal efficiency of Hg^0.

TABLE 2. Effect of Gas Components[a] in Flue Gas on Hg^0 Adsorption and Oxidation by Br_2 on Flyash[b] at 358 K

$[Br_2]_0$ (ppm)	flyash rank	Hg^0 half-life, $t_{1/2}$ (s)							
		N2	O2	H2O	CO	SO2	NO	HCl	mix
0	flyash-L	187	187	172	195	256	161		205
	flyash-B	194	194	188	194	215	183	28.8	29
13	flyash-L	16.5	16.5	16.1	16.5	18.1	15.8		17.6
	flyash-B	13.2	13.2	13	13.2	14.6	12.7	13	14.3

[a] The concentration of SO_2, NO, CO, HCl, O_2, and H_2O was 1200 ppm, 130 ppm, 130 ppm, 14.7 ppm, 7%, and 2%, respectively. "Mix" refers to the mixture of gases with concentrations mentioned above, under conditions without HCl in the case of flyash-L, and with HCl in the case of flyash-B. [b] The flyash in the reactor was about 0.7(±0.07) g stuck on 255 cm^2 reactor surface.

Flyash Induced Oxidation of Hg^0 by Br_2. The reactions follow pseudo-first-order kinetics with respect to the Hg^0 concentration. The half-life of Hg^0 was only 4.2 s for flyash-B and 4.8 s for flyash-L with 13 ppm Br_2 at 298 K. Comparing to the Hg^0 oxidation by 13 ppm Br_2 in the gas phase with a half-life of 33 s at 298 K and Hg^0 adsorption with a half-life of 157 s on flyash-B and 95 s on flyash-L at 298 K, the flyash induced Hg^0 oxidation by Br_2 with a half-life of less than 5 s clearly played the most important role in enhancing Hg^0 removal from flue gas.

The flyash induced oxidation rate of Hg^0 by Br_2 decreased with increasing temperatures. The half-life of Hg^0 increased from about 4.5 s at 298 K to 14.3 s for flyash-B and 17.6 s for flyash-L at 358 K. This is attributed to decreasing Br_2 adsorption capacities on flyash at high temperatures. Figure 3 compares the Hg^0 half-life on flyash-B, flyash-B0, flyash-L, and flyash-L0 to that on two PAC, Darco-Hg-LH, and Darco-Hg, at several temperatures. The flyash runs were performed using 13 ppm Br_2, whereas the PAC runs were without Br_2. The results indicate that the performance of flyash-B and flyash-L in the presence of 13 ppm Br_2 was comparable to that of Darco-Hg above 340 K, although they were much better at temperatures below 330 K. However, flyash containing no unburned carbon, e.g., flyash-B0 and flyash-L0, were much less effective in the Hg^0 removal (Figure 3). It is obvious that the unburned carbon in flyash plays a major role in the promotion of Hg^0 oxidation through the rapid adsorption of Br_2. Adsorbed Br_2 on carbon can effectively remove Hg^0 from the gas phase (*12*, *17*).

The effect of the amount of flyash in a gas volume on the Hg^0 oxidation by Br_2 was studied. Experiments were performed in three sizes of flasks coated with different amounts of flyash. For comparison, Darco-Hg-LH and Darco-Hg were tested under the same conditions except without Br_2 gas. The Hg^0 oxidation rates were correlated to the amount of flyash and gas volume according to the mass balance

$$-V\frac{d[Hg^0]}{dt} = k_s[Hg^0]M\epsilon \text{ or } -d[Hg^0]/dt = \frac{k_sM\epsilon}{V}[Hg^0] \quad (12)$$

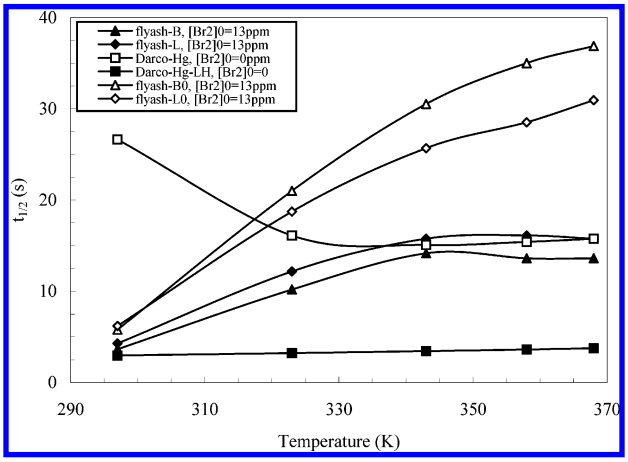

FIGURE 3. Comparison of Hg^0 removal rates by Powder activated carbon (Darco-Hg-LH and Darco-Hg) and flyash in combination with Br_2 gas at various temperatures. The Hg^0 removal rates (the smaller the half-life the better the removal rates) with Darco-Hg-LH was the best, while the Darco-Hg and flyash with 13 ppm Br_2 were comparable at temperatures above 340 K, although flyash-B was slightly better than flyash-L and Darco-Hg.

where V is the gas volume; M and ϵ are the amount and surface area of flyash, respectively; and k_s is the surface reaction rate constant. The half-life of Hg^0, $t_{1/2}$, in the gas phase can be expressed by eq 13 under the pseudo-first-order reaction condition.

$$t_{1/2} = 0.693/\left(\frac{k_s M\epsilon}{V}\right) \quad \text{or} \quad 1/t_{1/2} = \frac{k_s M\epsilon}{V}/0.693 \quad (13)$$

When the reciprocal of the Hg^0 half-life is plotted with M/V for flyash-B and flyash-L, a linear correlation with a slope of 0.137 $s^{-1}\cdot(mg/mL)^{-1}$ for flyash-B and 0.13 $s^{-1}\cdot(mg/mL)^{-1}$ for flyash-L is obtained (Figure 4a). The results indicate that the flyash-B is comparable to the flyash-L, based on the same amount of flyash per volume of gas, in promoting the Hg^0 oxidation by Br_2. The kinetics of surface reactions may be affected by the gas mixing, especially involving fast reaction and large reactor. However, the results obtained from three sizes of flasks mentioned above indicate that the gas mixing did not appear to make a significant contribution. When the same plot was made for the Darco-Hg and Darco-Hg-LH, slopes of 0.05 $s^{-1}\cdot(mg/mL)^{-1}$ and 0.53 $s^{-1}\cdot(mg/mL)^{-1}$, respectively, were obtained (Figure 4a). To compare sorbent effectiveness for Hg^0 capture, it is assumed that the sorbent utilization in the experiments is identical for the same sorbent and has a constant ratio between different sorbent.

The effect of the bromine concentration on flyash-induced Hg^0 oxidation was also studied. A linear relationship of $1/t_{1/2}$ versus $[Br_2]$ was obtained (Figure 4b), indicating that the rate constant is first order with respect to bromine concentration up to about 21 ppm. Hg^0 oxidation rate appears to level off with further increase of Br_2 concentration, as shown by the result at a concentration of 27.5 ppm in Figure 4b, a behavior accountable by an adsorption isotherm.

As mentioned above, the adsorption of Hg^0 on flyash was relatively slow. Conversely, the adsorption of Br_2 on flyash was a fast process under the experimental conditions employed. Therefore, the rate determining step for the capture of Hg^0 from gas phase appears to be the chemisorption of Hg^0 on the adsorbed Br_2 on unburned carbon in flyash. The reaction product, $HgBr_2$, is not likely to desorb to regenerate active sites due to its low volatility. However, flyash and Br_2 are in large excess compared to Hg^0, whether the product is desorbed or not should not affect the overall reaction rate.

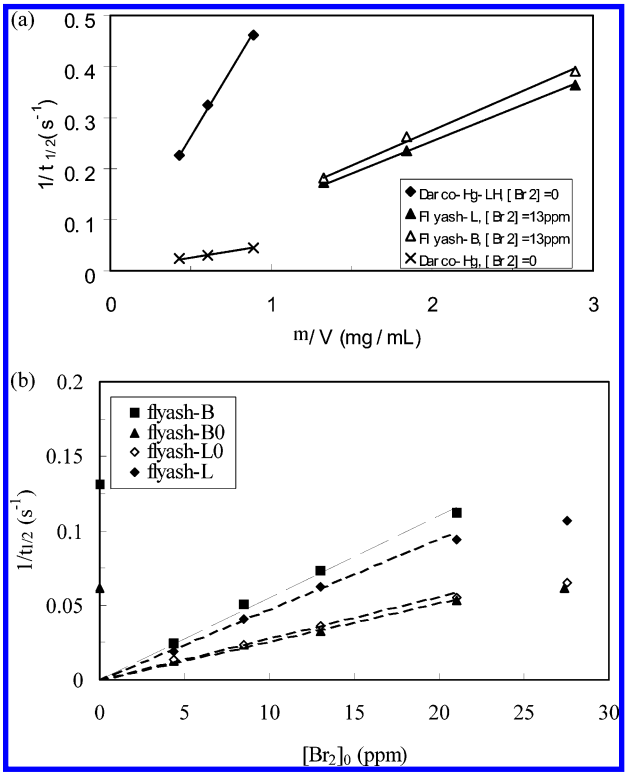

FIGURE 4. (a) A linear relationship of the reciprocal of the Hg^0 half-life vs the amount of sorbent at a given Br_2 concentration is indicative of first-order kinetics with respect to the sorbent concentration. (b). A linear relationship of the reciprocal of the Hg^0 half-life vs Br_2 concentrations, at a given sorbent concentration, is indicative of first-order kinetics with respect to the Br_2 concentration.

Effect of O_2, CO, H_2O, HCl, SO_2, and NO on Hg^0 Adsorption and Oxidation on Flyash. The effect of individual gases and their mixture on Hg^0 adsorption on flyash is listed in Table 2. O_2 and CO did not exhibit a detectable difference on the Hg^0 adsorption rate compared to N_2. H_2O vapor exhibited a promotion effect on the adsorption, but the effect dwindled with increasing temperatures. SO_2 inhibited the Hg^0 adsorption rate, which is attributed to the competition for the same adsorption sites on unburned carbons. Conversely NO promoted the Hg^0 adsorption rate. This could be attributed to an increase of active sites (*18*) on carbon particles as a result of the adsorption of molecules with an unpaired electron such as NO. The NO promotion effect decreased with increasing temperatures as the NO adsorption capacity dwindled (*18*). HCl enhanced Hg^0 adsorption the most among flue gas components. The half-life of Hg^0 was 45 s and 39 s with 14.7 and 29.3 ppm HCl, respectively, using flyash-L at 358 K. In the presence of a gas mixture containing SO_2, NO, CO, and H_2O, Hg^0 exhibited a small inhibition in adsorption (flyash-L in Table 2). From the aforementioned results, the Hg^0 half-life by the adsorption on flyash was too slow to make a significant removal of Hg^0 from flue gas, especially without HCl in the flue gas.

The effect of gases on flyash-induced Hg^0 oxidation by Br_2 is also shown in Table 2. Compared to the adsorption, the Hg^0 half-life decreased more than 1 order of magnitude with 13 ppm Br_2: 13.2 ± 0.1 s and 16.5 ± 0.2 s with flyash-B and flyash-L, respectively, at 358 K. O_2, CO, and H_2O did not show any detectable effect on the Hg^0 half-life compared to N_2. In a separated run, with 13 ppm Br_2, the half-life of Hg^0 remained relatively unchanged by the presence of 14.7 ppm HCl at 358 K. The Hg^0 half-life increased with increasing temperatures. SO_2 slightly inhibited the oxidation of Hg^0, and the half-life increased by about 8.4% with flyash-B and

10% with flyash-L at 358 K. NO, however, promoted the Hg^0 oxidation, and Hg^0 half-life decreased by 3.8% with flyash-B and 4.2% with flyash-L at 358 K. A simulated flue gas did not show a significant effect on Hg^0 oxidation. The Hg^0 half-life was 14.3 s with flyash-B and 16.5 s with flyash-L at 358 K.

Potential of Br_2 Gas for Enhancing Mercury Removal from Flue Gas. The flue gas stays in the duct downstream from air heaters for only a fraction of a second before reaching particulate collectors, where it resides typically for a period of less than 15 s. The temperatures of flue gas range from 390 K to 425 K in the duct and particulate collectors after air heaters. In this study, the kinetic data were obtained at temperatures below 363 K, a melting point limitation of HC. The estimation performed at temperatures above 363 K was done by the extrapolation.

Considering a case where the flue gas contains 50 ppm NO, based only on the gas-phase reaction pathway, then 52 ppm of Br_2 would be needed in the flue gas to convert 50% of Hg^0 to the oxidized form in 15 s at 410 K.

However, it is imperative to include the flyash contribution, as it is in the flue gas and can significantly accelerate Hg^0 oxidation by Br_2. The extrapolation of the kinetics of flyash promoted oxidation from the laboratory's batch system to the power plant's continuous system is difficult, not to mention that the properties of flyash and the flue gas conditions vary from plant to plant. Despite the difficulties in making an accurate prediction, a qualitative estimate of the Br_2 performance under flue gas conditions, i.e., flue gas containing all essential constituents, including SO_2, NO_x, CO, HCl, H_2O, and flyash, and at an appropriate temperature should be useful.

Darco-Hg-LH and Darco-Hg had been tested for mercury removal at a full scale coal-fired power plant (*2*) under continuous flow conditions, they were tested under the laboratory batch conditions, and the Hg^0 removal rates by two PAC were then used as the basis for predicting the performance of flyash induced Hg^0 removal by Br_2 in full scale systems. However, the prediction of Br_2 with flyash for Hg^0 capture cannot be done without making an assumption that the sorbent utilization in the laboratory experiments is identical for the same sorbent and has a constant ratio between different sorbent. Relative Hg^0 removal efficiencies by Darco-Hg-LH, Darco-Hg, and flyash with 13 ppm Br_2 obtained from the laboratory experiments are shown in Figure 3.

A linear relationship was obtained by plotting the reciprocal of the Hg^0 half-life versus M/V (Figure 4a), from which the Hg^0 removal efficiency can be more accurately estimated. The slope of the lines, representing incremental increase of the reciprocal of Hg^0 half-life per unit change of the M/V at 296 K, was 8.43, 0.803, 2.20, and 2.08 s^{-1} $(lb/ft^3)^{-1}$ for Darco-Hg-LH, Darco-Hg, flyash-B, and flyash-L, respectively. Based on these results, the Hg^0 removal efficiency by flyash with 13 ppm Br_2 was between Darco-Hg-LH and Darco-Hg at 296 K. However, flyash-B and flyash-L became less effective with increasing temperature until 343 K, when the efficiency stabilized (Figure 3). The efficiencies of Darco-Hg increased with increasing temperatures from 297 K to 330 K and maintained unchanged with further increase to 368 K. This behavior could be attributed to the fact that low temperature favored Hg^0 adsorption, and high temperature favored chemical reaction. The efficiencies of Darco-Hg-LH remained unchanged regardless of the changes of temperature (297−368 K). The Hg^0 removal efficiency by flyash with 13 ppm Br_2 was comparable to that of Darco-Hg above 340 K, when the amount of flyash was three times greater than the Darco-Hg.

In a demonstration (*2*) at the 140 MW Meramec Station, approximately 30% of particulate-bound and oxidized mercury in flue gas was measured. The total mercury removal efficiencies of 80% and 60% were obtained, respectively, by injecting Darco Hg-LH and Darco-Hg at a feed rate of 1.2 lb/MMacf. Assuming all of the particulate bound mercury was captured in the particulate collectors, about 71% and 43% of Hg^0 captured was obtained by Darco-Hg-LH and Darco-Hg, respectively. By increasing the feed rate to 3.2 lb/MMacf, the total mercury removal efficiency increased to 97% with Darco-Hg-LH and 70% with Darco-Hg, corresponding to a 96% and 57% Hg^0 captured by Darco-Hg-LH and Darco-Hg, respectively.

Considering a case when flue gas comprises 350 lb of flyash/MMacf (*19*) and by trading the Br_2 for flyash concentrations based on the first-order kinetics (Figure 4a,b), the flyash is estimated from the laboratory and field test results mentioned above to be able to achieve 43% Hg^0 oxidation with 0.12 ppm Br_2 and about 60% Hg^0 oxidation with 0.4 ppm Br_2 in flue gas. Hg^0 oxidation should increase with further increase of Br_2 concentration in flue gas. It must be emphasized that the above estimate is based on flyash-B and flyash-L that were received and assumes that their performance at flue gas temperatures (390−415 K) are identical to those between 340 K and 368 K. Not only the LOI but also the BET surface areas and the chemical property of the unburned carbon in flyash are the major factors that determine flyash's effectiveness in the promotion of Hg^0 oxidation by Br_2. Also, it must be emphasized that the estimate is of qualitative nature, and the actual performance of Br_2 gas injection approach cannot be accurately obtained until a scale-up demonstration is performed.

This study indicates that Br_2 introduced downstream from air heaters of coal-fired power plants can selectively oxidize Hg^0 atom to an oxidized form of mercury. The reactions of Br_2 with SO_2 and NO in flue gas are relatively slow such that the majority of Br_2 introduced is accessible for the reaction with Hg^0. Hg^0 oxidation in the gas phase was found to be less important than flyash-induced oxidation by Br_2. This study also demonstrates a new coal byproduct utilization method (*20*) involving in situ capturing of Hg^0 by flyash in a power plant system.

Extensive efforts (*2*, *7*, *21*) have been pursued to develop sorbents other than PAC for mercury capture because the PAC approach may have negative impact on flyash byproduct credits. The use of gas oxidant, such as bromine, with flyash as a sorbent could provide an alternative to the utility industry for effective mercury emission control.

Acknowledgments

We thank Brian Higgins and Guisu Liu of MobotecUSA for providing flyash samples. This work was supported by the Assistant Secretary for Fossil Energy, U.S. Department of Energy, under Contract DE-AC02-05CH11231 through the National Energy Technology Laboratory.

Note Added after ASAP Publication

This paper was published ASAP January 18, 2007. Errors in the author affiliation footnotes were corrected in the version published ASAP January 22, 2007.

Literature Cited

(1) Sloss, L. L. *Mercury − emissions and control*; CCC/58; IEA Coal Research: London, U.K., 43pp (Feb, 2002); ISBN 92-9029.-371-3.

(2) Feeley, T. J., III; Brickett, L. A.; O'Palko B. A.; Murphy, J. T. Field Testing of Mercury Control Technologies for Coal-Fired Power Plants, DOE/NETL Mercury R&D Program Review, May 2005.

(3) US-EPA, T6560-50.-P. Standards of Performance for New and Existing Stationary Source: Electric Utility Steam Generating Units, 40 CFR Parts 60, 63, 72 and 75, March 15, 2005. See http://www.epa.gov/ttn/atw/utility/utiltoxpg.html (accessed Dec 2006).

(4) Kellie, S.; Cao, Y.; Duan, Y.; Li, L.; Chu, P.; Mehta, A.; Carty, R.; Riley, J. T.; Pan, W. P. Factors Affecting Mercury Speciation in

a 100-MW Coal-Fired Boiler with Low-NOx Burners. *Energy Fuels* **2005**, *19*, 800−806.
(5) Bustard, J.; Renninger, S.; Chang, R.; Miller, R.; Monroe, L.; Sjostrom, S. Results of Activated Carbon Injection for Mercury Control Upstream of a COHPAC Fabric Filter. Presented at the A&WMA/EPA/DOE/EPRI Combined Power Plant Air Pollutant Control Mega Symposium, Washington, DC, May 19−22, 2003.
(6) Blythe, G.; Richardson, C.; Rhudy, R. Pilot Evaluation of the Catalytic Oxidation of Mercury for enhanced Removal in Wet FGD Systems. In Proceedings of Air Quality III: Mercury, Trace Elements, and Particulate Matter Conference, Arlington, VA, September 9−12, 2002. Energy and Environmental Research Center, University of Dakota, Grand Fork, North Dakota, Sept 2002.
(7) Granite, E. J.; Pennline, H. W.; Hargis, R. A. Novel Sorbents for Mercury Removal from Flue Gas. *Ind. Eng. Chem. Res.* **2000**, *39*, 1020−1029.
(8) Sliger, R. N.; Going, D. J.; Kramlich, J. C. Kinetic Investigation of the High-Temperature Oxidation of Mercury by Chlorine Species. Proceeedings of the Western States Section of the Combustion Institute, Fall 1998 Meeting, Seattle, Washington, October, 1998.
(9) Zumdahl, S. S.; Zumdahl, S. A. *Chemistry*; Houghton Mifflin Co.: Boston, MA 02116-3764; 2003.
(10) Ariya, P. A.; Khalizov, A.; Gidas, A. Reactions of Gaseous Mercury with Atomic and Molecular Halogens: Kinetics, Product Studies, and Atmospheric Implications. *J. Phys. Chem. A* **2002**, *106*, 7310−7320.
(11) Yan, N. Q.; Liu, S. H.; Chang, S. G.; Miller, C. Method for the Study of Gaseous Oxidants for the Oxidation of Mercury Gas. *Ind. Eng. Chem. Res.* **2005**, *44*, 5567−5574.
(12) Sun, W.; Yan, N. Q.; Jia, J. P. Removal of Elemental Mercury in Flue Gas by Brominated Activated Carbon. *China Environ. Sci.* **2006**, *26*, 257−261.
(13) Benson, S. W. *The Foundations of Chemical Kinetics*; McGraw-Hill Book Co., Inc.: New York, 1960.
(14) Lewis, G. N.; Randall, M.; Pitzer, K. S.; Brewer, L. *Thermodynamics*, 2nd ed.; McGraw-Hill Book Co.: New York, 1961.
(15) Hisatsune, I. C.; Zafonte, L. A Kinetic Study of Some Third-order Reactions of Nitric Oxide. *J. Phys. Chem.* **1969**, *73*, 2980−2989.
(16) Clark, A. *The Theory of Adsorption and Catalysis*; Academic Press: New York, 1970.
(17) Nelson, S.; Landreth, R.; Zhou, Q.; Miller, J. Accumulated Power-Plant Mercury Removal Experience with Brominated PAC Injection. Presented at the Combined Power Plant Air Pollution Control Mega Symposium, Washington, DC, Aug 30−Sept 2, 2004.
(18) Xia, B.; Phillips, J.; Chen, C.; Radovic, L. R.; Silva, I. F.; Menendez, J. A. Impact of Pretreatments on the Selectivity of Carbon for NO_x Adsorption/Reduction. *Energy Fuels* **1999**, *13*, 903−906.
(19) Soud, H. N.; Mitchell, S. C. *Particulate Control Handbook for Coal-Fired Plants*; IEACR/93; IEA Coal Research: London, U.K., July 1997; ISBN 92-9029-287-3.
(20) Wang, S.; Wu, H. Environmental-Benign Utilization of Fly Ash as Low-Cost Adsorbents. *J. Hazard. Mater.* **2006**, *B136*, 482−501.
(21) Lee, J. Y.; Ju, Y.; Keener, T. C.; Varma, R. S. Development of Cost-Effective Noncarbon Sorbents for Hg^0 Removal from Coal-Fired Power Plants. *Environ. Sci. Technol.* **2006**, *40*, 2714−2720.

Received for review July 17, 2006. Revised manuscript received November 23, 2006. Accepted November 27, 2006.

ES061705P